Journal of Zhejiang University-SCIENCE A (Applied Physics & Engineering)
ISSN 1673-565X (Print); ISSN 1862-1775 (Online)
www.zju.edu.cn/jzus; www.springerlink.com
E-mail: jzus@zju.edu.cn

Statistical extremes and peak factors in wind-induced vibration of tall buildings*

Ming-feng HUANG†[1], Chun-man CHAN[2], Wen-juan LOU[1], Kenny Chung-Siu KWOK[3]

([1]*Institute of Structural Engineering, Zhejiang University, Hangzhou 310058, China*)

([2]*Department of Civil and Environmental Engineering, Hong Kong University of Science and Technology, Hong Kong*)

([3]*School of Engineering, University of Western Sydney, NSW, Australia*)

†E-mail: mfhuang@zju.edu.cn

Received May 18, 2011; Revision accepted Sept. 27, 2011; Crosschecked Dec. 6, 2011

Abstract: In the structural design of tall buildings, peak factors have been widely used to predict mean extreme responses of tall buildings under wind excitations. Vanmarcke's peak factor is directly related to an explicit measure of structural reliability against a Gaussian response process. We review the use of this factor for time-variant reliability design by comparing it to the conventional Davenport's peak factor. Based on the asymptotic theory of statistical extremes, a new closed-form peak factor, the so-called Gamma peak factor, can be obtained for a non-Gaussian resultant response characterized by a Rayleigh distribution process. Using the Gamma peak factor, a combined peak factor method was developed for predicting the expected maximum resultant responses of a building undergoing lateral-torsional vibration. The effects of the standard deviation ratio of two sway components and the inter-component correlation on the evaluation of peak resultant response were also investigated. Utilizing wind tunnel data derived from synchronous multi-pressure measurements, we carried out a wind-induced time history response analysis of the Commonwealth Advisory Aeronautical Research Council (CAARC) standard tall building to validate the applicability of the Gamma peak factor to the prediction of the peak resultant acceleration. Results from the building example indicated that the use of the Gamma peak factor enables accurate predictions to be made of the mean extreme resultant acceleration responses for dynamic serviceability performance design of modern tall buildings.

Key words: Level-crossing rate (LCR), Wind-induced vibration, Mean extreme response, Combined resultant process, Peak factor method

doi:10.1631/jzus.A1100136 **Document code:** A **CLC number:** TU311.3; TU973

1 Introduction

Modern tall buildings are wind sensitive structures. Recent trends towards developing increasingly taller, irregular, and complex buildings imply that these structures are potentially undergoing excessive vibration during strong winds. Making accurate predictions of wind loads and dynamic effects on such high-rise structures is therefore a necessary step in the design process (Sun and Chen, 2000). For the past few decades, wind-tunnel testing has become the best practice method for measuring wind loads and analyzing wind-induced effects on tall buildings (Cermak, 2003). By means of either the high-frequency force balance (HFFB) or synchronous multi-pressure sensing system (SMPSS), aerodynamic wind loads can be estimated experimentally on a rigid scale model of the prototype. Based on the measured aerodynamic wind loading, the dynamic response of a building can then be calculated in the time or frequency domain.

Due to inherent random characteristics of wind, the wind-induced response of tall buildings is treated as a random process. For structural design purposes, the extreme values of a response process are of most

* Project supported by the National Natural Science Foundation of China (No. 51008275), and the China Postdoctoral Science Foundation (No. 201104736)

interest. Given the standard deviation of a response process, Davenport's peak factor (Davenport, 1964) is conventionally employed to estimate the expected or mean extreme value of wind-induced responses in wind engineering practice. Davenport (1964) showed that, if the underlying parent distribution of a response process is Gaussian, then the extreme values of the process will asymptotically follow a Gumbel distribution. For a zero-mean response process, the so-called peak factor can be defined as the ratio of the largest peak response to the standard deviation value of the response. In general, Davenport's peak factor provides satisfactory estimates of the maximum peak response for wide-band response processes, but it may yield conservative estimates for narrow-band response processes (Kareem, 1987; Gurley *et al.*, 1997). Vanmarcke (1972; 1975) improved the estimation of the first-passage probability for stationary Gaussian processes by taking into account the dependence of barrier crossings. He developed a formula for the probabilistic extreme value, the so-called Vanmarcke's peak factor, in terms of the shape parameter (bandwidth) of the power spectral density (PSD) of the underlying random response process. Unlike Davenport's peak factor, Vanmarcke's peak factor can be directly related to an explicit measure of the time-variant reliability and can be applicable to narrow-band response processes while taking consideration of the spectral bandwidth effects.

The use of Davenport's or Vanmarcke's peak factor for estimating the expected extreme responses of tall buildings to wind is based on the assumption that the underlying stochastic response is Gaussian. Such an assumption is valid for many general wind engineering applications. However, non-Gaussian wind effects may arise from specific but important situations, such as responses of a non-linear building system, turbulence-induced local pressure fluctuations on building surfaces, and combined resultant acceleration responses of a tall building. Previous studies on modeling of general non-Gaussian response processes focused mainly on the functional transformation of a standard Gaussian model (Grigoriu, 1984), or the use of series representation of distributions including Gram-Charlier and Edgeworth's series based on Hermite polynomials (Winterstein, 1988; Gurley *et al.*, 1997). The closed-form formula for the mean extreme of a non-Gaussian process was developed by Gurley *et al.* (1997) based on the Hermite model. But such Hermite model based approaches require the skewness and kurtosis of the fluctuating process, which always require time history information to estimate. Ochi (1988) presented an analytical development of the probability density functions (PDFs) for peaks and troughs of a non-Gaussian random process where the response of a non-linear system was represented in the form of a Volterra second-order functional series.

Specific efforts have been made to modify Davenport's peak factor for predicting non-Gaussian gusts and extreme effects (Winterstein, 1988; Sadek and Simiu, 2002; Holmes and Cochran 2003; Tieleman *et al.*, 2007). Sadek and Simiu (2002) presented an automated statistical procedure for estimating extreme peak distributions of wind-induced non-Gaussian internal forces in low-rise buildings by using the standard translation processes approach. Holmes and Cochran (2003) investigated the probability distributions of extreme pressure coefficients by statistically fitting the measured pressure data into a Gumbel distribution and a generalized extreme value distribution. Using the Sadek-Simiu procedure, Tieleman *et al.* (2007) estimated the extreme peak pressure distribution based on wind-induced time history pressure data recorded in a wind tunnel and determined the design pressure and load coefficients at any selected probability level of non-exceedance for reliability-based structural design.

In the dynamic serviceability design of tall buildings, the important system-level responses of interest are the component accelerations and their resultant acceleration responses at the corner of a tall building under wind excitations. The maximum resultant acceleration can be determined by combining the individually calculated or measured component maxima (Isyumov *et al.*, 1992; Melbourne and Palmer, 1992; Xie *et al.*, 2007; Chen and Huang, 2009). One conservative approach for predicting the maximum resultant acceleration is to combine two orthogonal component accelerations by taking the square-root-of-the-sum-of-the-squares (SRSS) of the two component peak responses. Such an approach gives an upper bound estimate of the maximum resultant acceleration response, thus resulting in an unduly conservative response prediction for the dynamic serviceability design of wind sensitive tall buildings. In the pursuit of a better estimate, Isyumov *et al.* (1992) developed an empirically derived joint action factor for accounting

for the interaction relationship between the maxima of two independent component responses based on experimental data. Although the use of the empirical joint action factor provides a practical means for estimating maximum resultant acceleration response, the approach was developed based on specific experimental data, and thus cannot guarantee improved accuracy. Recently, Chen and Huang (2009) proposed a practical combination scheme for evaluating peak resultant response based on a parametric study using various mathematical models.

This paper firstly revisits the mathematical analysis of the mean level-crossing rate (LCR) for a stationary random process and the previous work on peak factors in the context of first-passage probability. Vanmarcke's peak factor evaluated at various values of a bandwidth parameter is compared to Davenport's peak factor. The time-variant reliability design implication of Vanmarcke's peak factor is also highlighted. Secondly, based on the asymptotic theory of statistical extremes, the so-called Gamma peak factor can be obtained analytically for a non-Gaussian resultant response characterized by a Rayleigh distribution process. Using the Gamma peak factor, a combined peak factor method can then be developed for predicting the mean extreme resultant acceleration responses of tall buildings under wind excitations. Given the root-mean-square (RMS) values of acceleration components, the peak component and peak resultant acceleration responses of the Commonwealth Advisory Aeronautical Research Council (CAARC) building are calculated using Davenport's peak factor, Vanmarcke's peak factor and the Gamma peak factor. The peak acceleration values predicted by the peak factor methods are compared with the time history response maximum results obtained by time domain analysis using wind force data derived from synchronous multi-pressure measurements. Results of comparisons indicate that the mean extreme component and resultant accelerations can be accurately obtained by using Vanmarcke's peak factor and the Gamma peak factor.

2 Level-crossing rate in the analysis of first-passage probability

In this section, the mean LCR of a Gaussian process is revisited and that of a non-Gaussian process is then investigated. In order to consider the spectral bandwidth effect, Vanmarcke's peak factor is compared with the conventional Davenport's peak factor for the prediction of mean extremes of a Gaussian response process.

2.1 Mean level-crossing rate of a combined random process

Under wind excitation, a tall building may vibrate in a lateral-torsional manner such that the resultant response may involve several component responses in a 3D manner. For simplicity, a building floor is assumed to be a rigid diaphragm such that the floor moves in two sway components and one rotation around the floor center. Therefore, the total linear acceleration at the most distant corner (R_x, R_y) from the floor center of a building can be calculated as

$$a_{cx} = \ddot{x} - R_y\ddot{\theta},\ a_{cy} = \ddot{y} + R_x\ddot{\theta}, \tag{1}$$

where $\ddot{x}, \ddot{y}$ denote the two translational acceleration components and $\ddot{\theta}$ represents the torsional acceleration component at the floor center of the building. The resultant response at the building corner can then be obtained as $\sqrt{a_{cx}^2 + a_{cy}^2}$. Note that Gaussianity is valid for an acceleration component based on full-scale measurement data (Li *et al.*, 2010).

Assuming that the corner of a building experiences two perpendicular translational component responses, $X(t)$ and $Y(t)$, the combined resultant process can be rewritten as

$$A(t) = \sqrt{X^2(t) + Y^2(t)}. \tag{2}$$

If $X(t)$ and $Y(t)$ are two independent processes that follow a Gaussian distribution with a zero-mean and a common standard deviation of $\sigma_X = \sigma_Y$, then the resultant process $A(t)$ follows a Rayleigh distribution, which can be given as

$$f_A(a) = \frac{a}{\sigma_A^2}\exp\left(-\frac{a^2}{2\sigma_A^2}\right), \tag{3}$$

where σ_A denotes the mode value of $A(t)$. Since it is assumed that the two component processes have the

same standard deviation, the mode value of $A(t)$ coincides with the component standard deviation such that $\sigma_A = \sigma_X = \sigma_Y$. As shown by full-scale measurement data (Isyumov *et al.*, 1992), the actual peak resultant response deviates most from the SRSS combination of two individual peak components when $\sigma_X = \sigma_Y$. Since the most significant joint action between two component responses X and Y occurs when $\sigma_X = \sigma_Y$, it becomes necessary and useful to first investigate the joint action effects under the condition of two random component processes with equal fluctuating variation (i.e., $\sigma_X = \sigma_Y$) and then later to extend the investigation to more general cases where $\sigma_X \neq \sigma_Y$.

Taking the derivative on both sides of Eq. (2) with respect to t, we can obtain:

$$\dot{A}(t) = \frac{X(t)}{A(t)}\dot{X}(t) + \frac{Y(t)}{A(t)}\dot{Y}(t). \tag{4}$$

Since the derivatives of the Gaussian processes $X(t)$ and $Y(t)$ remain Gaussian, the time derivative process $\dot{A}(t)$ of the Rayleigh process $A(t)$ is deemed Gaussian if the derivative $\dot{A}(t)$ can be approximately regarded as a linear combination of $\dot{X}(t)$ and $\dot{Y}(t)$. Assuming that the derivative process $\dot{A}(t)$ is Gaussian, its PDF $f_{\dot{A}}(\dot{a})$ can then be expressed as

$$f_{\dot{A}}(\dot{a}) = \frac{1}{\sqrt{2\pi}\sigma_{\dot{A}}}\exp\left(-\frac{\dot{a}^2}{2\sigma_{\dot{A}}^2}\right), \tag{5}$$

where $\sigma_{\dot{A}}$ indicates the standard deviation value of the derivative process $\dot{A}(t)$. If the resultant process $A(t)$ is independent of its derivative process $\dot{A}(t)$, the joint PDF $f_{A,\dot{A}}(a,\dot{a})$ for calculating the mean LCR can be determined from Eqs. (3) and (5) as

$$\begin{aligned} f_{A,\dot{A}}(a,\dot{a}) &= f_A(a)f_{\dot{A}}(a) \\ &= \frac{a}{\sqrt{2\pi}\sigma_A^2\sigma_{\dot{A}}}\exp\left(-\frac{1}{2}\left(\frac{a^2}{\sigma_A^2}+\frac{\dot{a}^2}{\sigma_{\dot{A}}^2}\right)\right). \end{aligned} \tag{6}$$

Based on Rice's formula for the mean crossing rate, the mean upcrossing rate of level b for the Rayleigh process $A(t)$ can be obtained as

$$v_b^+ = \int_0^\infty \dot{a} f_{A,\dot{A}}(b,\dot{a})\mathrm{d}\dot{a} = \frac{b\sigma_{\dot{A}}}{\sqrt{2\pi}\sigma_A^2}\exp\left(-\frac{b^2}{2\sigma_A^2}\right). \tag{7}$$

According to Eq. (4), a simulation study was carried out to investigate the probabilistic distribution of $\dot{A}(t)$ by randomly sampling two component Gaussian processes using Monte Carlo simulations. Even when the combined resultant response $A(t)$ is a non-Gaussian Rayleigh process, its derivative $\dot{A}(t)$ was found, by means of the Kolmogorov-Smirnov goodness of fit test (KS test), to fit well to a Gaussian distribution (Clauset *et al.*, 2009) as long as the component processes of $A(t)$ are Gaussian.

2.2 Vanmarcke's peak factor

The largest peak response over a given time duration τ can be defined as a new random variable:

$$Y_\tau = \max\left\{|Y(t)|; 0 \le t \le \tau\right\}. \tag{8}$$

Let the first-passage time T_b be a random variable denoting the instant at which the structural absolute response $|Y(t)|$ first crosses the threshold level b. The largest absolute response does not exceed the threshold level b if, and only if, the corresponding first-passage time T_b does not occur within the time duration τ. Thus, the equivalence of the events $Y_\tau \le b$ and $T_b \ge \tau$ yields the fundamental relationship between the distributions of the largest value and the first-passage time (also the first-passage probability)

$$P[Y_\tau \le b] = P[T_b \ge \tau]. \tag{9}$$

For a prescribed probability p of the largest peak response being within the specific threshold over the time period τ, the corresponding response threshold denoted as $b_{\tau,p}$, can be obtained:

$$P(Y_\tau \le b_{\tau,p}) = p. \tag{10}$$

The ratio of $b_{\tau,p}/\sigma_Y$ determined by Eq. (10) can

be regarded as a kind of peak factor. Based on the fact that the largest extreme values of a Gaussian process asymptotically follow a Gumbel distribution, Davenport (1964) developed for practical use the following peak factor as the mean extreme normalized by the standard deviation of the process:

$$g_f = \sqrt{2\ln \nu_0 \tau} + \gamma / \sqrt{2\ln \nu_0 \tau}, \qquad (11)$$

where Euler's constant γ=0.5772. For a narrow-band resonant response, the mean zero-crossing rate ν_0 can be simply approximated by the natural frequency of a building, and the observation time duration τ is usually taken as 600 or 3600 s in wind engineering practice (Davenport, 1964; Gurley *et al.*, 1997). Davenport's peak factor is independent of a spectral bandwidth parameter. Based on the extreme value theory, the probability of the largest peak response not exceeding the expected maximum peak response can be evaluated by using the Type I extreme value distribution (or the Gumbel distribution) as

$$p = P(Y_\tau \le g_f \sigma_Y) = \mathrm{e}^{-\mathrm{e}^{-\gamma}} = 0.5704. \qquad (12)$$

Davenport's peak factor was developed under the assumption that the out-crossings constitute a Poisson model, which has been found to be too conservative when the response $Y(t)$ is a narrow-band process and the threshold level b is not high enough with respect to the RMS value of the response (Vanmarcke, 1975). Furthermore, the consecutive out-crossings of the response $Y(t)$, cannot be realistically assumed to be independent events, as generally they tend to occur in clumps. Vanmarcke (1975) developed a peak factor accounting for the dependence among the crossing events as

$$g_p \approx \sqrt{2\ln\left\{\frac{\nu_0 \tau}{\ln(1/p)}\left[1-\exp\left(-q^{1.2}\sqrt{\pi \ln\frac{\nu_0 \tau}{\ln(1/p)}}\right)\right]\right\}}, \qquad (13)$$

where $\nu_0 = \sigma_{\dot{Y}} / (\pi \sigma_Y)$, representing the mean zero-crossing rate of the Gaussian process $Y(t)$; $q = \sqrt{1-\lambda_1^2/(\lambda_0\lambda_2)}$ is a shape factor that characterizes the bandwidth of the process, in which the spectral moments λ_m can be defined as

$$\lambda_m = \int_0^\infty \omega^m G_Y(\omega)\mathrm{d}\omega,\ m = 0,1,2,4, \qquad (14)$$

where $G_Y(\omega)$ is a one-sided PSD function of the process and it can be shown that $\lambda_0 = \sigma_Y^2, \lambda_2 = \sigma_{\dot{Y}}^2$, and $\lambda_4 = \sigma_{\ddot{Y}}^2$.

The peak factors, calculated according to Davenport's peak factor given in Eq. (11) and Vanmarcke's peak factor of Eq. (13), are plotted as a function of ν_0 within the range of 0.1–1.1 Hz for typical multi-story building structures with several chosen values of bandwidth shape factor q (Fig. 1). For the comparison with the conventional Davenport's peak factor, Vanmarcke's peak factor has been given based on Eq. (13) with the probability of no exceedance p=0.5704 and an excitation duration time τ=3600 s. Davenport's peak factor is independent of the spectral bandwidth parameter q (Fig. 1), and always gives more conservative results, particularly for a narrow-band process with a smaller value of q. For a wide-band process with a value of q approaching 1, Vanmarcke's peak factor approaches the value of Davenport's peak factor.

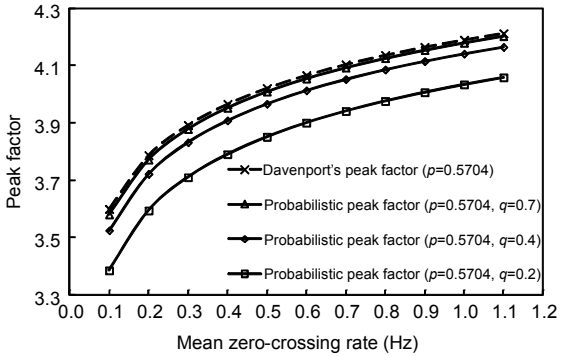

Fig. 1 Peak factors with spectral bandwidth parameter q (τ=3600 s)

Note that the mean extreme of the combined resultant process can be semi-analytically derived by

$$F_{A_\tau}(b) = P(A_\tau \le b) = \exp\left[-\frac{b\sigma_{\dot{A}}}{\sqrt{2\pi}\sigma_A^2}\tau\exp\left(-\frac{b^2}{2\sigma_A^2}\right)\right] \approx \exp\left[-\exp\left(-\frac{b-u_n}{\beta_n}\right)\right], \qquad (15)$$

where $F_{A_\tau}(b)$ denotes the cumulative probability distribution function of A_τ, which is defined as the largest resultant peak response over a given time duration τ; u_n and β_n are the location and scale parameters of the Type I Gumbel distribution; and the subscript n denotes the quantity or distribution parameter associated with a sample of peak response values with size n. Eq. (15) is based on the theory that the largest extreme values of a Gaussian process asymptotically approach a Gumbel distribution. The location and scale parameters u_n and β_n are empirically determined by linearly fitting $-\ln[-\ln(F_{A_\tau}(b))]$ as a function of b. Then, the mean extreme value is accordingly determined as

$$\mu_{A_\tau} = u_n + \gamma\beta_n. \tag{16}$$

However, Eqs. (15) and (16) give only an empirical way to determine the mean extreme value of the resultant response. The closed-form formula of mean extreme of resultant response will be developed below by investigating the peak distribution of a random process.

3 Peak distribution of a combined random process

Although the probability peak distributions of Gaussian processes have been extensively studied, there have been few studies of the probability distributions of peaks of non-Gaussian random processes (Ochi, 1998). In this section, a new analytical solution for the probability peak distribution of a non-Gaussian combined process is developed.

For a narrow-band process, each upcrossing event can possibly lead to a corresponding peak. The expected number of peaks above the given threshold level b per second can then be approximated by the level upcrossing rate v_b^+. If the desired peaks are counted by the peak-over-threshold approach (Cheng *et al.*, 2003), the expected number of total peaks per second can be well estimated from the mean upcrossing rate of a sufficiently small threshold level b, such as mode value σ_A. The probability peak distribution of a non-Gaussian combined process $A(t)$ can then be related to the mean LCR as

$$f_{A_m}(b) \approx -\frac{1}{v^+_{\sigma_A}}\frac{\mathrm{d}v_b^+}{\mathrm{d}b}, \tag{17}$$

where A_m denotes the local peak response value of the process $A(t)$.

Considering the Rayleigh resultant process $A(t)$ with the mean LCR v_b^+ given in Eq. (7), the probability peak distribution of the non-Gaussian combined process $A(t)$ can be obtained from Eq. (17) as

$$f_{A_m}(b) \approx \frac{1}{\sigma_A}\left(\frac{b^2}{\sigma_A^2}-1\right)\exp\left[-\frac{1}{2}\left(\frac{b^2}{\sigma_A^2}-1\right)\right],\ b \ge \sigma_A. \tag{18}$$

By introducing the intermediate threshold level $c = b^2/\sigma_A^2 - 1$ corresponding to a peak-dependent intermediate random variable $C = A_m^2/\sigma_A^2 - 1$, referred to as the intermediate peak variable, the elementary probability of the event for an occurring peak with $\{b \le A_m \le b+\mathrm{d}b\}$ is equal to the elementary probability of the event for the intermediate peak variable with $\{c \le A_m^2/\sigma_A^2 - 1 \le c+\mathrm{d}c\}$ as

$$f_{A_m}(b)\mathrm{d}b = \frac{c}{2\sqrt{c+1}}\exp(-c/2)\mathrm{d}c,\ c \ge 0. \tag{19}$$

Therefore, the PDF of the intermediate peak variable C can be expressed from Eq. (19) as

$$f_C(c) = \frac{c}{2\sqrt{c+1}}\exp(-c/2). \tag{20}$$

For wind related time-variant reliability problems, a desired threshold level b is normally larger than $3\sigma_A$ such that the intermediate threshold $c = b^2/\sigma_A^2 - 1$ is generally larger than 8. At the tail range of c where $c \ge 8$, the coefficient term $c/(2\sqrt{c+1})$ can then be replaced by $c/4$ on the conservative side such that the PDF of the intermediate peak variable C given in Eq. (20) can be approximated into a form of Gamma distribution, as

$$f_C(c) \approx \frac{c}{4}\exp(-c/2). \tag{21}$$

In general, the Gamma probability model of Eq. (21) results in a higher PDF value than that of the original PDF model of Eq. (20) at the tail range of intermediate peak variables, indicating a more conservative estimation of the crossing failure probability using the Gamma probability model given in Eq. (21). Fig. 2 shows the PDF curve of the intermediate peak variable and its corresponding Gamma probability model for a Rayleigh combined process with σ_A=1. The tail distribution behavior of the intermediate peak variable can be well approximated by the Gamma distribution. A similar tail-equivalent approach was used by Fujimura and Der Kiureghian (2007) for nonlinear random vibration analysis.

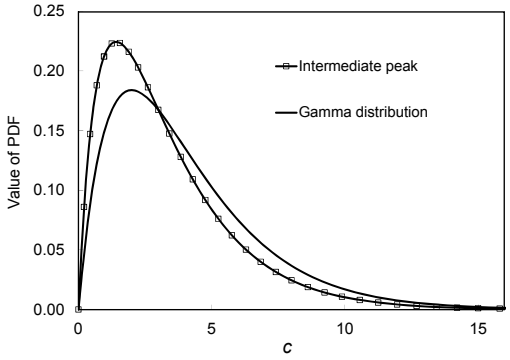

Fig. 2 PDFs of peaks and the intermediate peak variable of a Rayleigh process

4 Asymptotic extreme value distribution and the Gamma peak factor

From the viewpoint of the statistics of extremes, the largest peak or extreme values can be statistically obtained from a sample of peak response values Y_{m_i} with size n as

$$Y_n = \max\left\{Y_{m_1}, Y_{m2}, \ldots, Y_{m_n}\right\}, \tag{22}$$

where $Y_{m_1}, Y_{m_2}, \ldots, Y_{m_n}$ are assumed to be statistically independent and identically distributed with the same peak distribution. The mean value of Y_n, or the so-called expected maximum or mean extreme response, is a desired quantity essential for structural design against random vibration. The expected peak factor, widely used in wind engineering, can be defined as the ratio of the expected maximum response to the standard deviation value of the random response.

A closed-form expression of the peak factor for a combined resultant response process $A(t)=\sqrt{X^2(t)+Y^2(t)}$ with σ_X=σ_Y is first developed in this section. Based on the PDF of the intermediate peak variable $C = A_m^2 / \sigma_A^2 - 1$ in the form of the Gamma distribution given in Eq. (21), the corresponding CDF of C can be analytically obtained as

$$F_C(c) = P(C \le c) = 1 - (1 + c/2)\exp(-c/2),\ c \ge 0. \tag{23}$$

Since the extreme value arising from the Gamma PDF of C (i.e., Eq. (23)), converges asymptotically to the Type I Gumbel distribution, the location parameter u_n and the scale parameter β_n of the corresponding extreme value of the intermediate peak variable can be readily determined from the analytical distribution of C in Eq. (23) and the definitions of u_n and β_n (Huang *et al.*, 2009b),

$$\left(1+\frac{u_n}{2}\right)\exp\left(-\frac{u_n}{2}\right)=\frac{1}{n}. \tag{24}$$

$$\beta_n = [nf_C(u_n)]^{-1} = \left[n\frac{u_n}{4}\exp\left(-\frac{u_n}{2}\right)\right]^{-1}. \tag{25}$$

Based on the determinations of u_n and β_n, the mean value μ_{C_n} and standard deviation σ_{C_n} of the extreme value of the intermediate peak variable C can be evaluated, respectively, as

$$\mu_{C_n} = u_n + \gamma\beta_n = 2\ln n + 2\ln\ln n + \frac{2\gamma\sqrt{\ln n}}{\ln n + \ln\ln n}, \tag{26}$$

$$\sigma_{C_n} = \frac{\pi}{\sqrt{6}}\beta_n = \frac{\pi\sqrt{2\ln n}}{\sqrt{3}(\ln n + \ln\ln n)}. \tag{27}$$

Using the relationship of the intermediate peak variable C to the peaks of a Rayleigh process A_m, i.e., $C = A_m^2 / \sigma_A^2 - 1$, the expected peak factor of a combined resultant process with a Rayleigh distribution can be written as

$$g_G = \sqrt{\mu_{C_n} + 1} = \sqrt{2\ln n + 2\ln\ln n + \frac{2\gamma\sqrt{2\ln}}{\ln n + \ln\ln n} + 1}. \tag{28}$$

The above equation gives a closed-form formula for estimating the mean extreme response of a combined resultant process following the Rayleigh distribution. The expected peak factor determined by Eq. (28) is herein called the Gamma peak factor, which is derived from the Gamma distribution given in Eq. (21). For a narrow-band response process, one peak occurs possibly with one zero-crossing event. Therefore, the sample size of peaks as well as troughs, n, may be determined from the mean zero-crossing rate v_0 of the response process. Hence, for a given time duration τ, the sample size is taken as $n=v_0\tau$. The mean zero-crossing rate of the resultant process used in Eq. (28) can be determined from

$$v_0=\frac{1}{\pi}\frac{\sigma_{\dot{A}}}{\sigma_A}=\frac{\int_0^\infty \omega^2 G_A(\omega)\mathrm{d}\omega}{\pi\int_0^\infty G_A(\omega)\mathrm{d}\omega}, \tag{29}$$

where $G_A(\omega)$ is a one-sided PSD function of the resultant process.

The analytical Gamma peak factors for the resultant acceleration processes can be plotted as a function of the mean zero-crossing rate (Fig. 3). The Gamma peak factor consistently gives a value about 15% larger than that of Davenport's peak factor. Since the peak distribution of the resultant process according to Eq. (17) is defined for those peaks over the threshold of mode value σ_A, the expected maximum resultant response can then be estimated in terms of the Gamma peak factor and the mode value of the resultant process $A(t)$ as

$$\mu_{A_n}=g_G\sigma_A. \tag{30}$$

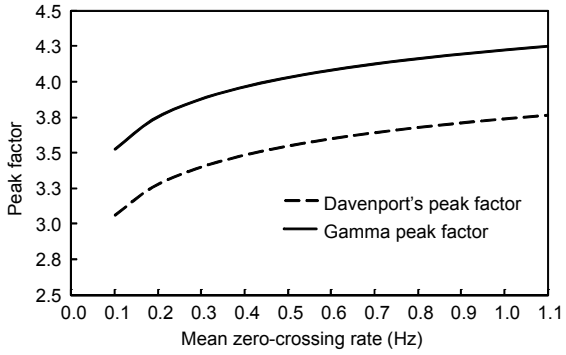

Fig. 3 Gamma peak factors for peak resultant accelerations (τ=600 s)

5 Peak factor method

In the dynamic serviceability design of tall buildings, it is important to predict the expected peak component and resultant acceleration response under random wind excitation. An accurate analytical closed-form formula given in Eq. (30) can be used to calculate the expected maximum resultant acceleration response of a tall building. Eq. (30), however, is obtained for the resultant process with two components having the same standard deviation. If two components do not have the same value of standard deviation, i.e., $\sigma_X\neq\sigma_Y$, the combined resultant process $A(t)$ will have a probability distribution model involving an integral expression which is more complicated than the analytical Rayleigh distribution. Assuming that two component responses $X(t)$ and $Y(t)$ follow a zero-mean Gaussian distribution, a reduced resultant process can be defined as

$$\tilde{A}(t)=\sqrt{\left(\frac{X(t)}{\sigma_X}\right)^2+\left(\frac{Y(t)}{\sigma_Y}\right)^2}. \tag{31}$$

Since the probability characteristic of $\tilde{A}(t)$ can be described by a Rayleigh distribution with a mode value of unity, the expected largest or mean extreme response of $\tilde{A}(t)$ can then be obtained from Eq. (30) as

$$\mu_{\tilde{A}_n}=g_G. \tag{32}$$

The actual resultant process can be rewritten in terms of $Y(t)$ and $\tilde{A}(t)$ as

$$A^2(t)=\tilde{A}^2(t)\sigma_X^2+Y^2(t)(1-\sigma_X^2/\sigma_Y^2). \tag{33}$$

Without loss of generality, we now discuss the resultant response from the component processes $X(t)$ and $Y(t)$ with $\sigma_X\leq\sigma_Y$. Assume that A_n attains its mean when the reduced resultant process $\tilde{A}(t)$ and the dominating component process $Y(t)$ simultaneously reach their mean peak values of g_G and $g_f\sigma_Y$, respectively. Substituting $\tilde{A}=g_G$ and $Y=g_f\sigma_Y$ into Eq. (33), the mean extreme resultant response of the combined process $A(t)$ can then be approximated as

$$\mu_{A_n} \approx \sqrt{(g_G^2 - g_f^2)\sigma_X^2 + g_f^2\sigma_Y^2}. \quad (34)$$

The use of Eq. (34) for predicting the peak resultant acceleration response can be referred to as the combined peak factor (CPF) method. The assumption of a full correlation between $Y(t)$ and $\tilde{A}(t)$ makes Eq. (34) somewhat conservative in the prediction of the peak resultant acceleration response of a building.

A practical resultant peak acceleration of a tall building can be computed by multiplying the empirical joint action factor (Isyumov *et al.*, 1992) and the fully correlated SRSS value of the peak resultant acceleration response as

$$\mu_{A_n} \approx \phi\sqrt{g_f^2\sigma_X^2 + g_f^2\sigma_Y^2}, \quad (35)$$

where ϕ is the empirical joint action factor, which may be given by an ellipsoid interaction formula as

$$\phi = 0.7 + 0.3\sqrt{1-(\sigma_X/\sigma_Y)^2},\ \sigma_X < \sigma_Y. \quad (36)$$

Note that the empirical joint action factor ϕ has a value ranging between 0.7 and 1, depending on the standard deviation ratio of the smaller component to the larger component acceleration response. A larger value of the ratio of two component responses implies a smaller value of the empirical joint action factor, and vice versa. For comparison purposes, using Eq. (35) to calculate the peak resultant acceleration response is regarded as the empirical joint action (EJA) method.

A correlation-dependent combination (CDC) method was proposed by Chen and Huang (2009) for evaluating the peak resultant response due to correlated response components as

$$\mu_{A_n} = \max\{\mu_{A\max 1}, \mu_{A\max 2}\}, \quad (37)$$

where

$$\mu_{A\max 1} = \sqrt{\frac{g_f^2(\sigma_X^2+\sigma_Y^2)}{2} + \sqrt{\frac{g_f^4(\sigma_X^2-\sigma_Y^2)^2}{4} + \rho_{XY}^2(g_f^2\sigma_X^2)(g_f^2\sigma_Y^2)}}, \quad (38)$$

$$\mu_{A\max 2} = 0.8\sqrt{g_f^2\sigma_X^2 + g_f^2\sigma_Y^2}, \quad (39)$$

where ρ_{XY} denotes the inter-component correlation coefficient between the X-direction and Y-direction response components. Note that even for a tall building with a 1D mode shape in each primary direction, two translational response components at the most distant corner (R_x, R_y) from the reference center of the building are correlated to a certain degree due to the torsional component of building motion as

$$\rho_{XY} = (R_X R_Y \sigma_{0\theta}^2)/(\sigma_{0x}\sigma_{0y}), \quad (40)$$

where σ_{0s} (s=x,y,θ) represents the standard deviation response components at the reference center of the building.

For comparison among various methods for evaluating peak resultant responses (i.e., the CPF method using Eq. (34), the EJA method using Eq. (35) and the CDC method using Eq. (37), and the conventional SRSS combination method), a joint action reduction factor can be defined as

$$\varphi = \mu_{A_n}/\sqrt{g_f^2\sigma_X^2 + g_f^2\sigma_Y^2}, \quad (41)$$

where the mean extreme resultant response μ_{A_n} can be evaluated using different methods. When μ_{A_n} is calculated by the EJA method according to Eq. (35), the joint action reduction factor φ is reduced to the empirical joint action factor ϕ.

Fig. 4 shows the joint action reduction factor φ as a function of σ_X/σ_Y and ρ_{XY} with n=$\nu_0\tau$=200 for a relatively short duration of 600 s using different methods including the EJA, CDC and the proposed analytical CPF methods. When using the CDC method, Eq. (37) has been evaluated at eight different correlation coefficients taken from 0 to 1 corresponding to the eight curves of the joint action reduction factor given in Fig. 4. When two component responses are more strongly correlated with $\rho_{XY}\geq 0.75$, the joint action reduction factor is found to be somewhat insensitive to the ratio of σ_X/σ_Y (Fig. 4). For buildings in which the inter-component responses are not strongly correlated such that $\rho_{XY}\leq 0.5$, the joint action reduction factor decreases steadily with the standard deviation ratio σ_X/σ_Y approaching unity, but varies insignificantly with the different values of ρ_{XY} (Fig. 4). As a result, the inter-component correlation coefficient ρ_{XY}

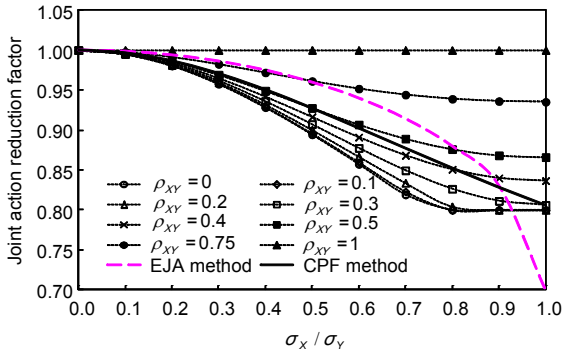

Fig. 4 Joint action reduction factor evaluated using various methods with a short time duration of 600 s

has a small influence on the peak resultant response particularly when $\rho_{XY} \leq 0.5$. It can be concluded that the mean extreme resultant response is more sensitive to the standard deviation ratio while being insensitive to the inter-component correlation for a tall building with weakly or even moderately correlated component responses.

The EJA method and our proposed CPF method are both independent of the inter-component correlation coefficient. Therefore, these two methods are easier to apply since they do not require more complicated evaluations of inter-component correlations, which generally depend on not only the modal frequencies and damping ratios, but also the cross PSD of modal forces (Huang *et al.*, 2009a). When the ratio σ_X/σ_Y is close to unity, the EJA method tends to underestimate the peak resultant response when compared to the CDC method using Eq. (37) and the CPF method using Eq. (34). The proposed CPF method is able to give a slightly more conservative response than the more accurate CDC method in cases where $\rho_{XY} \leq 0.3$ (Fig. 4). For most tall buildings where the component responses are normally not strongly correlated, i.e., $\rho_{XY} \leq 0.5$, the CPF method provides a straight forward analytical means for accurately predicting the peak resultant responses by properly estimating the joint action effects of component responses. Note that when a tall building with a highly irregular geometric shape does exhibit strong inter-component correlations, it becomes necessary to calculate the inter-component correlation coefficients and to apply the CDC method using Eq. (37) to predict the corresponding peak resultant response.

6 Application on the mean extreme wind-induced acceleration of tall buildings

6.1 The 45-story CAARC building

A 45-story steel tall building example (Fig. 5) is used to illustrate the use of various methods in the evaluation of peak resultant acceleration responses. Specifically, the application of Vanmarcke's peak factor in Eq. (13) and the Gamma peak factor in Eq. (28) together with the combined peak factor method is demonstrated to predict the peak component acceleration and peak resultant acceleration, respectively, of the building.

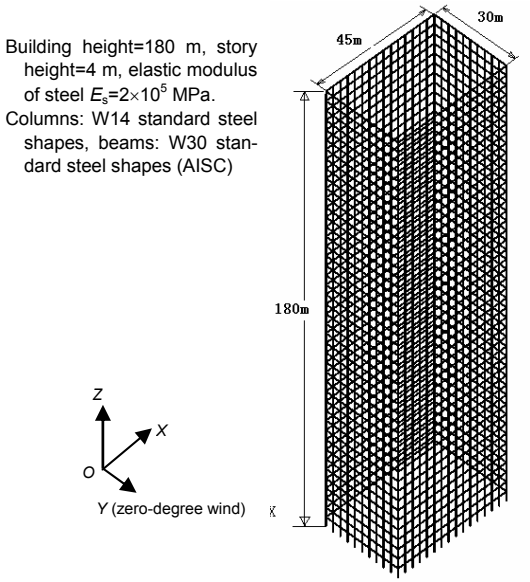

Fig. 5 A 3D view of the 45-story CAARC building

With a story height of 4 m and a bay width of 3 m, the 10-bay-by-15-bay 45-story steel framework (Fig. 5) has an overall height of 180 m and rectangular floor plan dimensions of 30 m by 45 m. The building has the same geometric shape as the CAARC standard tall building, which has long been used for calibration purposes using different wind tunnels (Wardlaw and Moss, 1970; Melbourne, 1980). The wind tunnel test was conducted at the China Light and Power (CLP) Wind/Wave Tunnel Facility of the Hong Kong University of Science and Technology (HKUST). Aerodynamic wind forces acting on a rigid 1:400 scale model of the building were measured using a synchronous multi-pressure sensing system (SMPSS) technique. The SMPSS consists of 14 ESP-16HD pressure scanner modules, which are able to measure

simultaneously local surface pressures on the model through a total of 216 pressure-taps. The model was installed with 6 layers of pressure-taps over its height with 36 pressure-taps in each layer. Each pressure-tap was connected to one of 16 ports of an ESP-16HD pressure scanner with a 750 mm single lumen PVC tube of 1.5 mm internal diameter, without any restrictor. Surface pressures were measured at a sampling frequency of 400 Hz, which was sufficient to measure pressure fluctuations with frequencies up to 2 Hz at the prototype scale. The SMPSS had been calibrated carefully so as to ensure that simultaneous pressure measurements were made possible to acquire accurately the correlation of pressure fluctuations for the building model.

The boundary layer wind model corresponding to a countryside open terrain (Category 2) in the wind code (AS/NZS 1170.2: 2002) was simulated in the wind tunnel. The power law exponents of the mean wind speed profile and the turbulence intensity profile were approximately 0.15 and −0.18, respectively. The mean wind velocity, turbulent intensity, turbulence length scale and Reynolds number are listed in Table 1 for the wind-tunnel scale model and the full scale prototype, respectively. A 10-year return period hourly mean wind velocity of 34.7 m/s at the reference height of 90 m in Hong Kong was used in the scale prototype.

Structural members were to be designed using the American Institute of Steel Construction (AISC) standard steel sections as follows: W30 shapes for beams and W14 shapes for columns (e.g., structural steel W flange section W14×159 means a section with 14 inch depth and a line density of 159 1b/ft, 1 inch =25.4 mm, 1 1b/ft=1.488 kg/m). For ease of construction, the columns on each vertical column line were grouped together to have a common section over three adjacent stories, while the corner beams of the exterior frame were grouped together to have the same section on each floor, as were the beams near the centre of each face of the building. The initial member sizes were established on the basis of a preliminary strength check. Along the height of the building, the columns and beams were divided into five different zones (Table 2). The natural frequencies of the building structure were found to be 0.197 Hz for the 1st mode, 0.251 Hz for the 2nd mode and 0.422 Hz for the 3rd mode. The zero-degree wind perpendicular to the wide face acting in the short direction (i.e., along the *Y*-axis) of the building was considered in the wind-induced dynamic response analysis. Based on the synchronous pressure measurement data, a time-stepping integration method was used to obtain the time histories of wind-induced response in the CAARC building example. A modal damping ratio of 1.5% of critical damping was used in the analysis.

6.2 Results and discussion

The bandwidth parameter q of the random acceleration response process is required for capturing the spectral effects on Vanmarcke's peak factor using Eq. (13). The PSD curves corresponding to the *X*-direction and *Y*-direction acceleration components at the top corner of the building can be obtained by spectral analysis (Fig. 6). For the PSD curve of *Y*-component acceleration, the first translational modal frequency (0.197 Hz, the vibration mode swaying in the *Y*-direction), the torsional modal frequency (0.422 Hz), and the second and third

Table 2 Structural member sizes of for the 45-story CAARC steel framework

Floor zone	Column	Beam
37F–45F	W14×159	W30×211
28F–36F	W14×257	W30×261
19F–27F	W14×370	W30×292
10F–18F	W14×500	W30×326
1F–9F	W14×550	W30×357

Table 1 Elevation and wind characteristics at different levels in model and prototype scales

Level	Elevation (m)		Mean velocity (m/s)		Turbulence length scale (m)		Reynolds numbers		Turbulent intensity (%)
	Model	Prototype	Model	Prototype	Model	Prototype	Model	Prototype	
1	0.0560	22	9.7	22.7	0.26	104.0	5.0×10^4	4.7×10^7	15.91
2	0.1688	68	11.5	27.0	0.34	137.0	6.0×10^4	5.6×10^7	12.20
3	0.2813	113	12.6	29.5	0.39	155.7	6.6×10^4	6.1×10^7	10.20
4	0.3375	135	13.0	30.5	0.41	162.9	6.8×10^4	6.3×10^7	9.48
5	0.3937	157	13.4	31.4	0.42	169.3	7.0×10^4	6.5×10^7	8.88
6	0.4359	174	13.7	32.0	0.43	173.7	7.1×10^4	6.7×10^7	8.48

Y-direction translational modal frequencies (0.544 Hz and 0.935 Hz, respectively) clearly indicate four corresponding resonant peaks. The second translational mode (0.251 Hz with swaying along the *X*-direction of the building) did not contribute noticeable resonant effects in the *Y*-direction acceleration response spectrum. Similarly, three noticeable resonant peaks corresponding to the first *X*-sway mode (0.251 Hz), the torsional mode (0.422 Hz) and the second *X*-sway mode (0.673 Hz) can be found in the *X*-component acceleration spectrum (Fig. 6).

Based on the acceleration response spectra, various orders of spectral moments can be computed by numerical integration, and the bandwidth parameter defined by the spectral moments can be evaluated. The bandwidth measure q was found to be 0.315 and 0.495 for *X*-directional and *Y*-directional component accelerations, respectively. Vanmarcke's peak factors and the peak component acceleration results are shown in Table 3. The peak factors for the prediction of mean extreme acceleration responses were calculated based on a given time duration of τ=600 s. As adopted in the Hong Kong Code of Practice (2004), the mean-crossing rate of vibration of the CAARC building was taken as its first modal frequency ν_0=0.197 Hz to determine the sample size $n=\nu_0\tau$ of peaks for two component acceleration processes. To ensure consistency with Davenport's peak factor, the probability of no exceedance p was taken as 57%. It was found that the peak *X*-component acceleration evaluated using the corresponding Vanmarcke's peak factor gave a value −4.2% lower than that calculated using Davenport's peak factor. One advantage of Vanmarcke's peak factor is that the extreme component responses can be evaluated at different levels of non-exceedance probability.

Table 4 presents the predicted extreme *X*-direction responses corresponding to various Vanmarcke's peak factors g_p evaluated at different levels of non-exceedance probability, i.e., from 35% to 95%. Due to different implications of time-variant reliability associated with various non-exceedance probabilities, the predicted probabilistic peak accelerations in Table 4 yield noticeable percentage differences ranging from −11% to 17% when compared to the mean extreme component response calculated using Davenport's peak factor. Such an advantage for predicting extreme response at different levels of time-variant reliability or non-exceedance probability may be useful in the context of reliability performance-based design of tall buildings.

Table 5 presents the peak resultant acceleration results at the top corner of the CAARC building. The

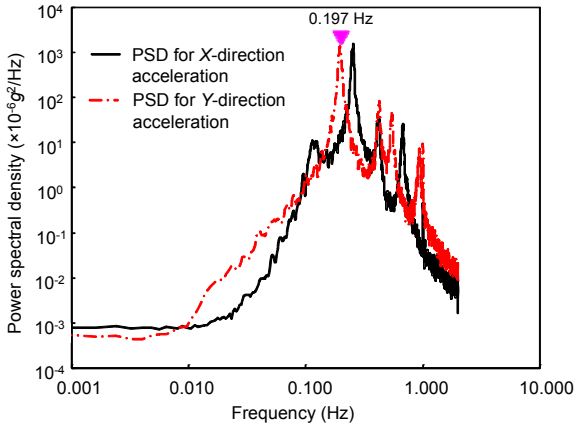

Fig. 6 PSD of acceleration responses for the CAARC building under zero-degree wind

Table 4 Extreme *X*-direction component accelerations at different levels of non-exceedance probability

Standard deviation	p	Peak factor		Peak acceleration ($\times10^{-3}g$)	
		g_f	g_p	$g_f\sigma$	$g_p\sigma$
5.1	35%	3.276	2.913	16.71	14.86 (−11%)
5.1	57%	3.276	3.133	16.71	15.98 (−4%)
5.1	65%	3.276	3.220	16.71	16.42 (−2%)
5.1	75%	3.276	3.349	16.71	17.08 (2%)
5.1	85%	3.276	3.522	16.71	17.96 (8%)
5.1	95%	3.276	3.846	16.71	19.61 (17%)

Note: The numbers in brackets represent the percentage difference of peak component acceleration values calculated using Vanmarcke's peak factor g_p compared with the values obtained using Davenport's peak factor g_f

Table 3 Component accelerations in the 45-story building under zero-degree wind

Component	Standard deviation	q	p	Peak factor		Peak acceleration ($\times10^{-3}g$)	
				g_f	g_p	$g_f\sigma$	$g_p\sigma$
X-direction	5.1	0.315	57%	3.276	3.133	16.71	16.0 (−4.2%)
Y-direction	5.1	0.495	57%	3.276	3.213	16.71	16.4 (−1.8%)

Note: The numbers in brackets represent the percentage difference of peak component acceleration values calculated using Vanmarcke's peak factor g_p compared with the values obtained using Davenport's peak factor g_f

Table 5 Peak resultant accelerations in the 45-story building under zero-degree wind

Peak resultant acceleration ($\times10^{-3}g$)				Used parameter			
Conventional SRSS method	CPF method Eq. (34)	EJA method Eq. (35)	CDC method Eq. (37)	g_f	g_G	ϕ	ρ_{XY}
23.5	19.6 (−17%)	16.5 (−30%)	18.8 (−20%)	3.276	3.751	0.7	0.067

Note: the numbers in brackets represent the percentage reduction of resultant acceleration values calculated using the CPF method, the EJA method or the CDC method compared with the value obtained using the conventional SRSS method

mean extreme resultant acceleration was calculated using four methods, i.e., the conventional SRSS method, the EJA method using Eq. (35), the CPF method using Eq. (34), and the CDC method of Eq. (37). The upcrossing rate of the resultant process used to determine the Gamma peak factor was calculated from Eq. (29) as 0.296 Hz. The conventional SRSS method resulted in the most conservative estimation of the mean extreme resultant acceleration response (Table 5). Using an empirical joint action factor of 0.7 with the standard deviation ratio $\sigma_X/\sigma_Y=1$, the EJA method resulted in a peak resultant acceleration of $16.5\times10^{-3}g$, which is 30% lower than the $23.5\times10^{-3}g$ calculated using the conventional SRSS method. With an inter-component correlation coefficient of $\rho_{XY}=0.067$, which is relatively small due to the symmetric building having predominantly 1D mode shapes, the CDC method gave a peak resultant acceleration of $18.8\times10^{-3}g$, indicating a 20% reduction from the conventional SRSS value. For this building, with the same standard deviation of two response components and weakly coupled inter-component responses, the CDC method actually degenerated into the simple 80% rule as given in Eq. (39). The proposed combined peak factor method resulted in a peak resultant acceleration of $19.6\times10^{-3}g$, which is only slightly larger (4.2%) than that of the CDC method, but 17% less than that of the conventional SRSS method.

The peak component acceleration and peak resultant acceleration presented in Tables 3 and 5 can also be verified by the expected maximum response values determined statistically through samples of component acceleration and resultant acceleration response histories obtained from the time history analysis of the CAARC building. Fig. 7 shows the time histories of the resultant acceleration responses at the top corner of the CAARC building together with the predicted peak resultant acceleration values delineated by the horizontal threshold lines. The total

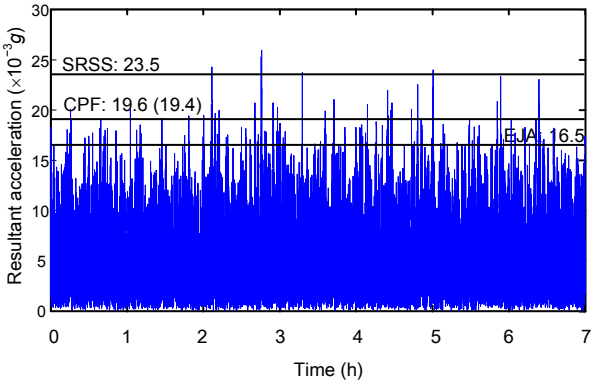

Fig. 7 Time histories resultant acceleration responses at the top corner of the CAARC building (the values in brackets are statistically estimated)

duration of time history data was taken to be 7 h, in which 42 samples of 10-min acceleration data records were obtained. The expected maximum resultant accelerations were statistically computed by averaging the 42 observed maximum resultant peaks over 42 samples of 10-min resultant acceleration data records. The mean extreme resultant response was statistically computed to be $19.4\times10^{-3}g$. The statistical result indicates that the proposed CPF method gave the encouraging prediction of $19.6\times10^{-3}g$ with only a 1% error. The 80% rule proposed by Chen and Huang (2009) also gave a comparable result of $18.8\times10^{-3}g$ with about a 3% error. While the conventional SRSS method overestimated the mean extreme resultant response by 21%, the EJA method underestimated the mean extreme value by 15%.

Note that the application of the CPF method does not require time history analysis of wind-induced responses of tall buildings. If only the RMS values of two component responses are available, Eq. (34) can be used to predict the peak resultant acceleration response of tall buildings. The RMS values of component acceleration responses (σ_{0s} ($s=x,y,\theta$)) can be conveniently obtained by frequency-domain analysis using wind force spectral information following the

wind codes or determined from the high frequency base balance test in the wind tunnel (Huang *et al.*, 2009a). The level of correlation between two acceleration components (X and Y) can also be assessed by Eq. (40). If the inter-component correlation coefficient ρ_{XY} is relatively small, i.e., $\rho_{XY}\leq 0.5$, the application of the CPF method is then recommended.

7 Conclusions

After reviewing the peak factor theory in random process, this paper presents the development of the Gamma peak factor by investigating probabilistic extreme values of random processes and the wind-induced response of tall buildings. Vanmarcke's peak factor, explicitly expressed in terms of the non-exceedance probability and the spectral bandwidth shape parameter, is compared with the conventional Davenport's peak factor for the prediction of mean extremes of a Gaussian response process. For a narrow-band response process, the use of Davenport peak factor without accounting for spectral bandwidth effects yields a conservative estimate of the mean extreme component response. Vanmarcke's peak factor has an advantage in that it may be used to predict extreme response at different levels of time-variant reliability or non-exceedance probability, which may be useful in the context of reliability performance-based design of tall buildings.

Using the asymptotic theory of statistical extremes, the Gamma peak factor has been obtained for a non-Gaussian combined resultant response characterized by a Rayleigh distribution process. Based on the Gamma peak factor, the combined peak factor method has been proposed for predicting the mean extreme resultant acceleration response of wind-sensitive tall buildings. The 45-story CAARC building tested in the wind tunnel was used to demonstrate the applicability of the combined peak factor method for evaluating the mean extreme resultant response. The wind tunnel derived acceleration time history results of the building verify that the combined peak factor method gives a reasonably accurate prediction of the mean extreme resultant acceleration responses when compared with the conventional SRSS method and the empirical joint action method.

The effects of the inter-component correlation on the evaluation of peak resultant response were also investigated with the aid of the correlation-dependent combination method. The mean extreme resultant response was found to be more sensitive to the standard deviation ratio of two sway components while being insensitive to the inter-component correlation for tall buildings which normally exhibit weakly or moderately correlated component responses. Compared with the correlation-dependent combination method, the combined peak factor method independent of inter-component correlation gives a convenient and yet accurate analytical means for predicting peak resultant response of wind sensitive tall buildings. To predict the extreme resultant response at different non-exceedance probability levels, further research is needed to improve the proposed combined peak factor method.

References

Cermak, J.E., 2003. Wind-tunnel development and trends in applications to civil engineering. *Journal of Wind Engineering and Industrial Aerodynamics*, **91**:355-370. [doi:10.1016/S0167-6105(02)00396-3]

Chen, X., Huang, G., 2009. Evaluation of peak resultant response for wind-excited tall buildings. *Engineering Structures*, **31**:858-868. [doi:10.1016/j.engstruct.2008.11.021]

Cheng, P.W., van Bussel, G.J.W., van Kuik, G.A.M., Vugts, J.H., 2003. Reliability-based design methods to determine the extreme response distribution of offshore wind turbines. *Wind Energy*, **6**:1-22. [doi:10.1002/we.80]

Clauset, A., Shalizi, C.R.,, Newman, M.E.J., 2009. Power-law distributions in empirical data. *SIAM Review*, **51**(4):661-703. [doi:10.1137/070710111]

Davenport, A.G., 1964. Note on the Distribution of the Largest Value of a Random Function with Application to Gust Loading. Proceedings, Institution of Civil Engineering, **28**(2):187-196.

Fujimura, K., Der Kiureghian, A., 2007. Tail-equivalent linearization method for nonlinear random vibration. *Probabilistic Engineering Mechanics*, **22**:63-76. [doi:10.1016/j.probengmech.2006.08.001]

Grigoriu, M., 1984. Crossing of non-Gaussian translation process. *Journal of Engineering Mechanics, ASCE*, **110**(4):610-620.

Gurley, K.R., Tognarelli, M.A., Kareem, A., 1997. Analysis and simulation tools for wind engineering. *Probabilistic Engineering Mechanics*, **12**(1):9-31. [doi:10.1016/S0266-8920(96)00010-0]

Holmes, J.D., Cochran, L.S., 2003. Probability distribution of extreme pressure coefficients. *Journal of Wind Engineering and Industrial Aerodynamics*, **91**:893-901. [doi:10.1016/S0167-6105(03)00019-9]

Hong Kong Code of Practice, 2004. Code of Practice on Wind Effects in Hong Kong. Buildings Department, Hong Kong.

Huang, M.F., Chan, C.M., Kwok, K.C.S., Hitchcock, P.A., 2009a. Cross correlation of modal responses of tall buildings in wind-induced lateral-torsional motion. *Journal of Engineering Mechanics, ASCE*, **135**(8):802-812. [doi:10.1061/(ASCE)0733-9399(2009)135:8(802)]

Huang, M.F., Chan, C.M., Kwok, K.C.S., Lou, W.J., 2009b. A Peak Factor for Predicting Non-Gaussian Peak Resultant Response of Wind-Excited Tall Buildings. Proc. the Seventh Asia-Pacific Conference on Wind Engineering, Taipei, Taiwan.

Isyumov, N., Fediw, A.A., Colaco, J., Banavalkar, P.V., 1992. Performance of a tall building under wind action. *Journal of Wind Engineering and Industrial Aerodynamics*, **41-44**: 1053-1064. [doi:10.1016/0167-6105(92)90112-N]

Kareem, A., 1987. Wind effects on structures: a probabilistic viewpoint. *Probabilistic Engineering Mechanics*, **2**:166-200.

Li, Q.S., Zhi, C.H., Duan, Y.D., Kao, C.S., Su, S.C., 2010. Full-scale measurements and analysis of wind-induced response of Taipei 101 Tower. *Journal of Building Structures*, **31**(3):24-31 (in Chinese).

Melbourne, W.H., 1980. Comparison of measurements of the CAARC standard tall building model in simulated model wind flows. *Journal of Wind Engineering and Industrial Aerodynamics*, **6**:78-88. [doi:10.1016/0167-6105(80)90023-9]

Melbourne, W.H., Palmer, T.R., 1992. Accelerations and comfort criteria for buildings undergoing complex motions. *Journal of Wind Engineering and Industrial Aerodynamics*, **41-44**:105-116. [doi:10.1016/0167-6105(92)90398-T]

Ochi, M.K., 1998. Probability distribution of peaks and troughs of non-Gaussian random process. *Probabilistic Engineering Mechanics*, **13**(4):291-298. [doi:10.1016/0266-8920(94)90017-5]

Sadek, F., Simiu, E., 2002. Peak non-Gaussian wind effects for database-assisted low-rise building design. *Journal of Engineering Mechanics, ASCE*, **128**(5):530-539. [doi:10.1061/(ASCE)0733-9399(2002)128:5(530)]

Sun, B.N., Chen, S.F., 2000. Wind-induced stochastic response of controlled tall buildings by complex-mode. *Journal of Zhejiang University SCIENCE*, **1**(4):421-426.

Tieleman, H.W., Ge, Z., Hajj, M.R., 2007. Theoretically estimated peak wind loads. *Journal of Wind Engineering and Industrial Aerodynamics*, **95**:113-132. [doi:10.1016/j.jweia.2006.05.004]

Vanmarcke, E.H., 1972. Properties of spectral moments with applications to random vibration. *Journal of Engineering Mechanics*, **98**(EM2):425-446.

Vanmarcke, E.H., 1975. On the distribution of the first-passage time for normal stationary random processes. *Journal of Applied Mechanics*, **42**:215-220.

Wardlaw, R.L., Moss, G.F., 1970. A Standard Tall Building Model for the Comparison of Simulated Natural Winds in Wind Tunnels. Report CC-662 Tech. 25, Commonwealth Advisory Aeronautical Research Council, UK.

Winterstein, S.R., 1988. Nonlinear vibration models for extremes and fatigue. *Journal of Engineering Mechanics, ASCE*, **114**(10):1772-1790.

Xie, J.M., Haskett, T., Kala, S., Irwin, P., 2007. Review of Rigid Building Model Studies and Their Further Improvements. Proc. 12th International Conference on Wind Engineering, Cairns, Australia, p.1175-1182.

2010 JCR of Thomson Reuters for *JZUS-A* and *JZUS-B*

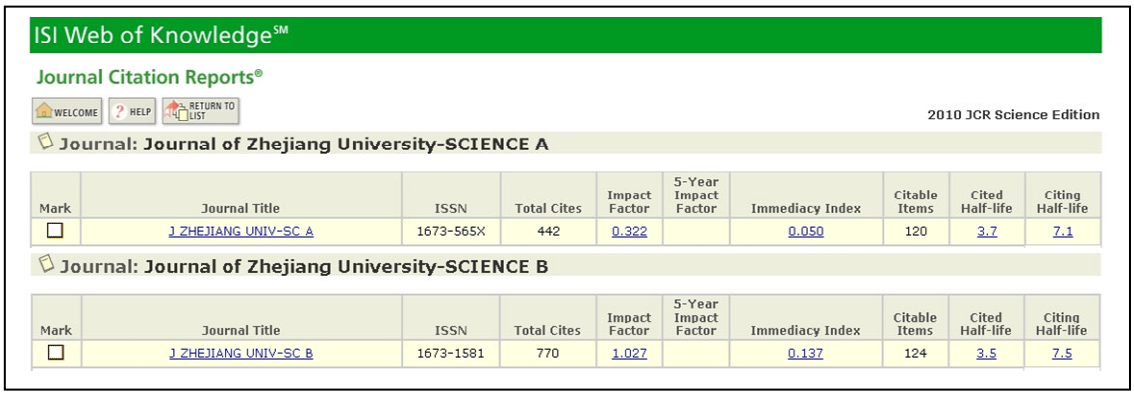

ISI Web of Knowledge℠

Journal Citation Reports®

WELCOME HELP RETURN TO LIST

2010 JCR Science Edition

Journal: Journal of Zhejiang University-SCIENCE A

Mark	Journal Title	ISSN	Total Cites	Impact Factor	5-Year Impact Factor	Immediacy Index	Citable Items	Cited Half-life	Citing Half-life
☐	J ZHEJIANG UNIV-SC A	1673-565X	442	0.322		0.050	120	3.7	7.1

Journal: Journal of Zhejiang University-SCIENCE B

Mark	Journal Title	ISSN	Total Cites	Impact Factor	5-Year Impact Factor	Immediacy Index	Citable Items	Cited Half-life	Citing Half-life
☐	J ZHEJIANG UNIV-SC B	1673-1581	770	1.027		0.137	124	3.5	7.5